Field Stabilization Study For TESLA

A. Mosnier and J.-M. Tessier
DAPNIA/SEA, CE Saclay, 91191 Gif/Yvette, France

Abstract

The beam energy spread at the exit the TESLA linac must be below the energy acceptance of the final focus but also small enough to limit the emittance dilution due to chromatic and dispersive effects. The intra-bunch energy spread, resulting from the rf sinusoidal wave and the induced bunch wake potential, can be reduced to about 5.10^{-4}, by running properly the bunch off the crest of the accelerating wave [1]. Any cavity field fluctuation, in phase and in amplitude, during the beam pulse will generate some bunch-to-bunch energy spread. It would be desirable to keep this energy spread below the intra-bunch energy spread in order to assure that the bunch-to-bunch chromatic effects will be no worse than the single bunch ones. The Lorentz forces (also called "radiation pressure") and microphonics, by shifting the cavity frequency, are the main bunch-to-bunch energy spread sources. With superconducting cavities operating in pulsed mode, the Lorentz Forces problem arises from the wall deformation response time [2] . The cavity frequency goes on to shift after the field rise time, whereas the beam is passing through the cavity. After a brieve review of the two methods [3,4] coping with the Lorentz forces detuning when one cavity only is fed by one klystron, the effect of parameters spreads is studied when several cavities are fed by one klystron. External feedback loops to minimize the residual amplitude and phase errors are then added and the loop gains are determined. The influence of a spread in external Qs (from coupler tolerances or on purpose for having different fields from cavity to cavity) is analysed and the extra power needed to stabilize the total accelerating voltage is given after an optimization of the beam injection time. Finally, microphonics effects, which can increase dramatically the field errors, are considered and a remedy, allowing to alleviate the problem, is proposed.

1. INTRODUCTION

During the field rise time, the generator frequency must be locked in any case on the cavity frequency which is shifting because of the Lorentz forces. The phase lock can be provided by a voltage controlled oscillator (VCO) or a self-excited loop. In a first method [3] the generator frequency is then suddenly switched to the reference frequeny (1300 MHz) as soon as the beam is injected into the cavity, leading to a frequency jump at the beam injection time. In a secong method [4] uses the self-exciting loop principle during the field rise time and during the beam pulse, without any frequency jump. The equations related to both methods and for one or several cavities per klystron can be found in Appendix 1. The principle of both methods can be described by the figure 1, showing the resonance frequency shift and the resulting phase fluctuation in case of one cavity for one generator.

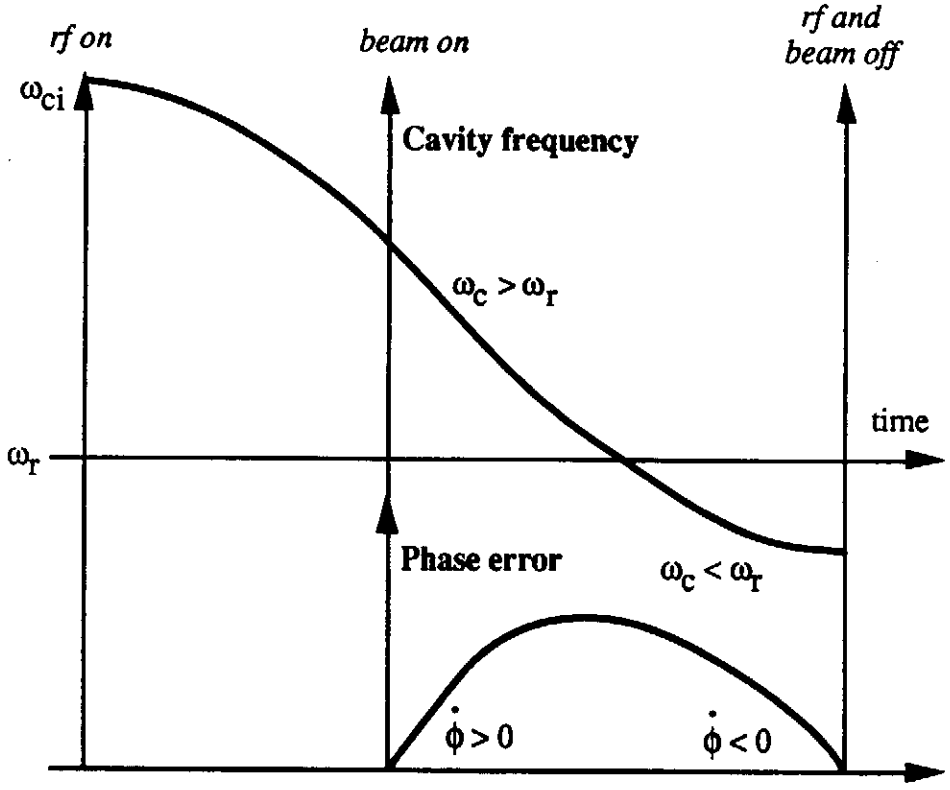

Figure 1 : Cavity frequency shift and phase variation

Whatever the method, the variation law of the cavity frequency, which changes quadratically with the field level, is completely determined during the rise time, but also during the beam pulse, because the field amplitude is assumed to stay approximately constant. The resonance frequency starts to shift down from an initial frequency detuning ω_{ci} . Assuming the phase error is zero at the beam injection time, the slope of the phase error is simply given by $\dot{\phi} = \omega_{c(t)} - \omega_r$. To minimize the phase shift during the beam traversal, the cavity frequency ω_c must hence be higher at the beginning (positive phase slope) and lower (negative phase slope) at the end than the reference frequency ω_r. The

optimal initial cavity detuning ω_{ci} is then entirely determined. The figure 2 gives the cavity frequency shifts and the phase errors evolutions for the TESLA cavity parameters when the initial cavity frequency has been adjusted to give the minimal phase variation.

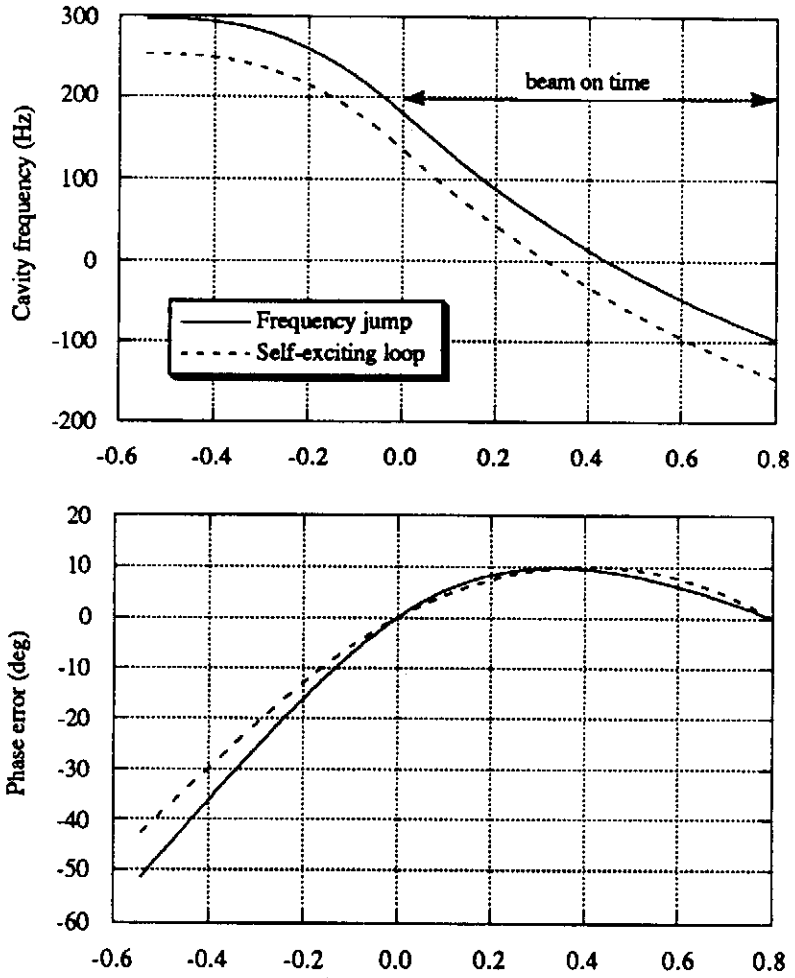

Figure 2 : Cavity frequency and phase error for both methods

If we look however in more details into the equations (see Appendix 1), small correction terms have to be added (the source is assumed matched to the beam load) :

$$\dot{\phi} = (\omega_{c(t)} - \omega_r) - \frac{1}{\tau}\frac{A_b}{A}\sin\phi \qquad \text{for frequency jump}$$

$$\dot{\phi} = (\omega_{c(t)} - \omega_r) + \frac{1}{\tau}\frac{A_b}{A}\sin\phi \qquad \text{for self - exciting loop}$$

where A and A_b are the field and beam amplitudes respectively

The sign difference in the correction terms explains why the initial detuning has to be slightly lower for the self-excited loop case (250 Hz instead of 300 Hz). The results for the Tesla Test Facility and for the TESLA parameters are summarized below.

1.1. simulations results with TTF parameters

The input parameters retained for TTF are listed in the following table 1

Accelerating Gradient	15 MV/m
Beam current	8 mA
electric time constant τ_e	0.78 ms
mechanical time constant τ_m	1 ms
beam injection time τ_e ln2	0.54 ms
beam pulse duration	0.8 ms
detuning parameter K	1 Hz/(MV/m)^2

Table 1 : parameter list for TTF

For each simulation, the initial cavity detuning df_0 and the initial rf phase ϕ_0 at the beginning of the rf power pulse are adjusted in order to cancel the phase deviation when the beam is injected and to minimize the phase error during the beam pulse. Table 2 gives the relative amplitude errors $\Delta V/V = (V_{max}-V_{min})/V$, the phase errors $\Delta\phi = \phi_{max}-\phi_{min}$ as well as the optimal initial detuning for both methods.

method	df_0 (Hz)	$\Delta V/V$ (10^{-3})	$\Delta\phi$ (deg)
Self-excited loop	90.34	0.74	3.58
Frequency jump	106.97	0.69	3.53

Table 2 : relative amplitude errors and phase errors with TTF parameters

The figures 3 and 4 show the corresponding curves of the amplitude and phase of the accelerating field.

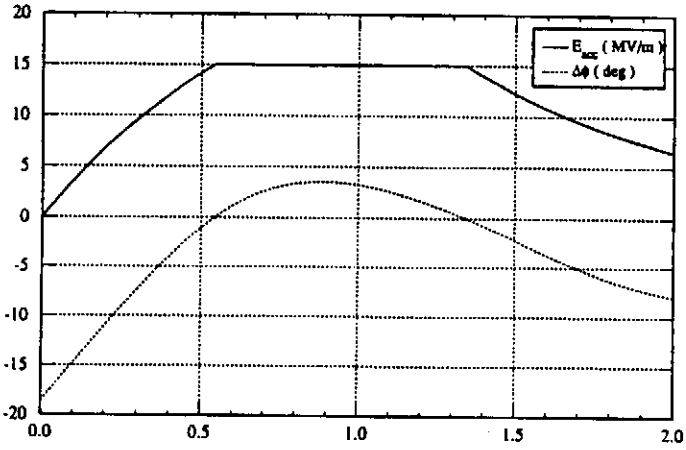

Figure 3 : amplitude and phase of the accelerating field (frequency jump)

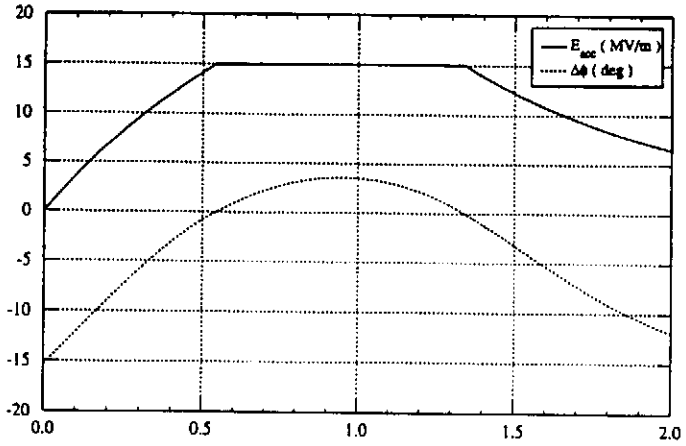

Figure 4 : amplitude and phase of the accelerating field (self-excited loop)

1.2. simulations results with TESLA parameters

The larger accelerating field foreseen for the TESLA linac (25 MV/m) will provide a larger detuning effect. Table 3 gives the results.

method	df_0 (Hz)	$\Delta V/V$ (10^{-3})	$\Delta\phi$ (deg)
Self-excited loop	251.60	5.76	10.03
Frequency jump	296.20	5.24	9.72

Table 3 : relative amplitude errors and phase errors with TESLA parameters

We conclude that both methods give very similar results. In the aim to reduce the cost of the rf power sources for TESLA, at least 16 cavities will be driven by one big klystron. Since the rf and mechanical parameters of the cavities will not be identical, the effect of a spread in the different parameters has to be studied.

2. SEVERAL CAVITIES FED BY ONE GENERATOR

The schematic layout and the equations of this multi-cavity rf system can be found in Appendix A. During the field rise time, the generator frequency has to be locked on the changing cavity frequency, but this locking can be carried out by using the phase signal either from one cavity voltage or from the vectorial sum of all cavity voltages. During the beam on time, the cavities chain can be driven either by a constant frequency generator (frequency jump method) or by means of a self-excited loop. There are therefore 4 different methods, which are summarized in the table 4.

signal from	a single cavity	vectorial sum of all cavities
self-excited loop	1	2
frequency jump	3	4

Table 4 : The 4 different methods

2.1. Initial detuning spread effect

When a spread in initial detunings is introduced, large phase and amplitude errors are expected when the frequency generator tracks the frequency of single cavity. Assuming for example an initial detuning error with respect to the optimal value of one cavity, typically ± 40 Hz (corresponding to a tuning angle error of 10°), the figure 5 shows the relative amplitude errors for the 4 methods with different detuning values. The frequency locking on a single cavity (methods 1 and 3) must be clearly rejected. The frequency locking on the vectorial sum signal with the self-excited loop or with the frequency method (methods 2 and 4) give satisfaying results up to large detuning error magnitudes and will be solely kept for the further studies.

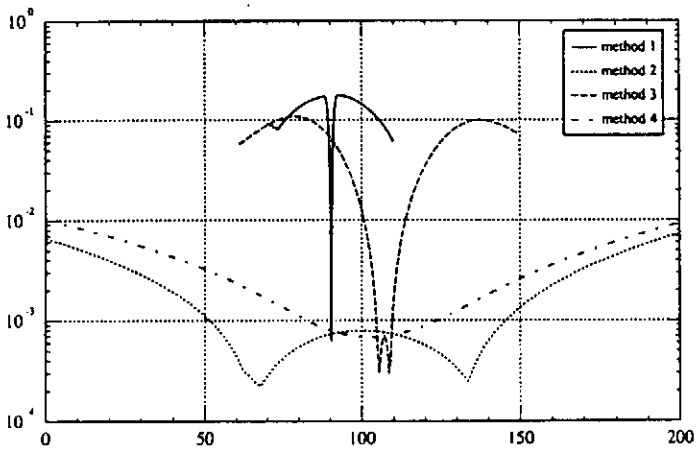

Figure 5 : relative amplitude error versus initial detuning error of a cavity

2.2. Simulation results for a chain of 16 cavities

For a given parameters spread, the results vary according to the errors taken for the calculation. We carry therefore out statistical calculations by varying randomly some parameters around the optimal values which minimize the amplitude and phase errors. The phase error is cancelled at the beam injection time for each simulation. Table 5 gives the mean and standard deviation of amplitude and phase errors for both methods (2 and 3) for a spread in the initial detuning, a spread in detuning parameter K and mechanical constant τ_m simultaneously, and a spread in the external Q. The results are given for an accelerating gradient of 15 MV/m and for 1000 different seeds of the random generator. The figures 6, 7 and 8 show the corresponding histograms. For a gradient of 15 MV/m and a detuning parameter K of 1 Hz/(MV/m)^2, we conclude that there is no dramatic performance degradation when a spread in initial cavity tuning or in simultaneous detuning parameter K and mechanical constant τ_m is introduced. We note that the self-exciting loop method provides slightly better results in amplitude fluctuation whereas the frequency jump method provide slightly better results in phase fluctuation. We check simply the general rule, which states that the self-exciting loop arrangement is more stable in amplitude.

parameter dispersion	method	$\langle \Delta V/V \rangle$ (10^{-3})	$\sigma_{\Delta V/V}$ (10^{-3})	$\langle \Delta\phi \rangle$ (deg)	$\sigma_{\Delta\phi}$ (deg)
df_0	SEL	3.25	1.19	4.92	1.15
(± 40 Hz)	FJ	4.81	1.03	3.97	0.35
K, τ_m	SEL	0.95	0.40	4.30	0.70
(± 20%)	FJ	2.00	0.45	3.80	0.25
Q_{ex}	SEL	14.92	2.48	4.63	0.15
(± 20%)	FJ	15.75	2.44	3.85	0.04

Table 5: amplitude and phase errors for various parameters spreads
(SEL and FJ mean self-excited loop and frequency jump methods)

It is worthwhile stressing that the cavity tuning error is assumed static because the starting phase has been adjusted in the simulations. This assumption is obviously not valid when the cavity detunings originate from mechanical vibrations. The effect of dynamic cavity tuning errors caused by microphonics will be studied in Chapter 4. On the other hand, external Q variations lead to large amplitude errors, which are essentially caused by the source-beam load mismatching. We will show in Chapter 3.3 how to minimize this effect, after having studied the control problem.

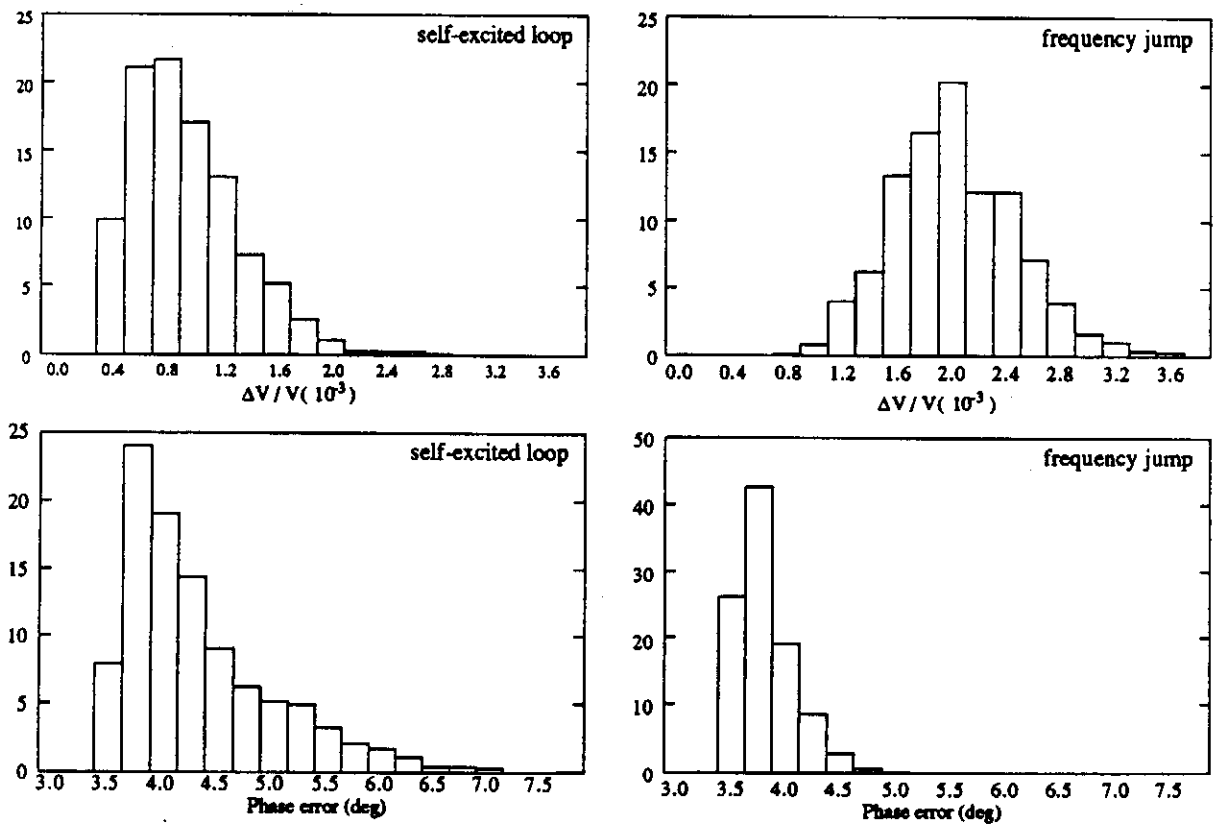

Figure 6: amplitude and phase histograms for a K and τ_m spread

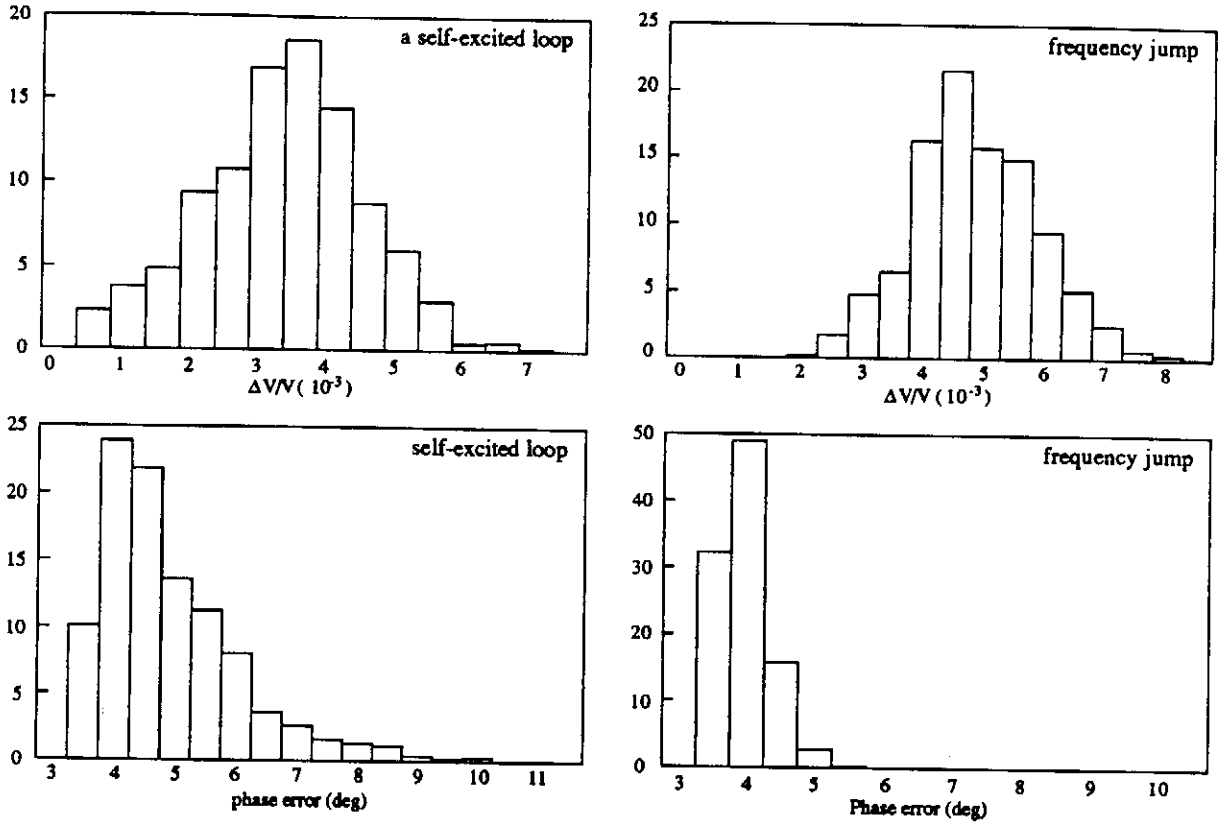

Figure 7: amplitude and phase histograms for a static cavity tuning error

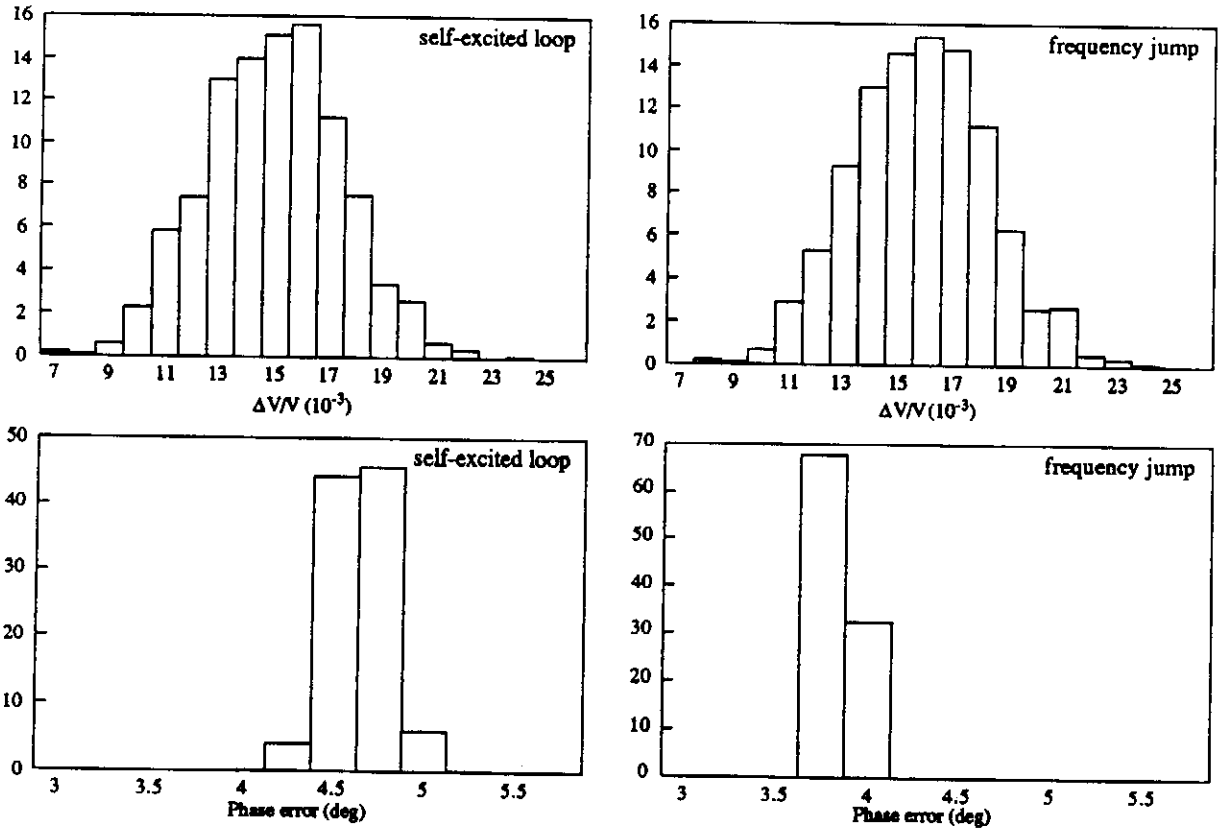

Figure 8: amplitude and phase histograms for a Qex spread

3. AMPLITUDE AND PHASE CONTROL

Feedback loops will stabilize the field, which is perturbated either by the Lorentz forces detuning or by microphonics detuning. Whatever the method, the feedback will control the total voltage $Ae^{j\phi}$. of the cavity chain during the beam pulse. A schematic drawing of the system and the additional equations are given in Appendix

3.1. Loop gains determination for one cavity

The task of the control system consists in reducing the bunch-to-bunch energy spread to the 10^{-4} level, but the needed extra rf power, in peak and in average power, must also stay within a reasonable level. We have then to determine the feedback loop gains, which will minimize the amplitude and phase errors with the minimal additional power. Since the reactive power provided by the phase loop only is efficient to stabilize the field, the phase loop gain G_ϕ was varied whereas the initial cavity tuning was optimized for each gain value. The plots 9 and 10 show the resulting peak and average extra power and the energy spread for a cavity operating at 25 MV/m with a self-excited loop and perturbated by the Lorentz forces.

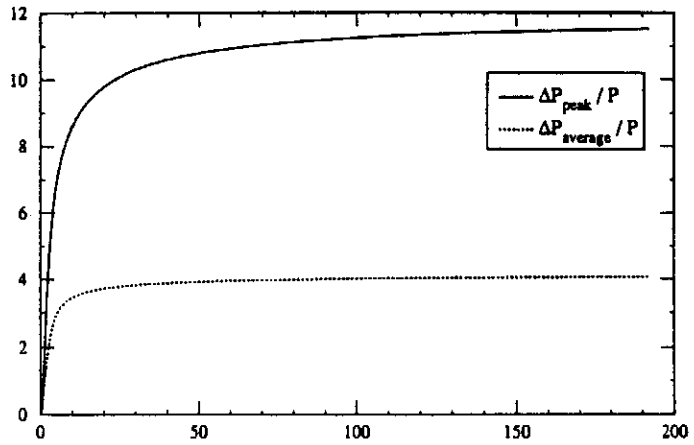

Figure 9 : Extra rf power vs the phase loop gain

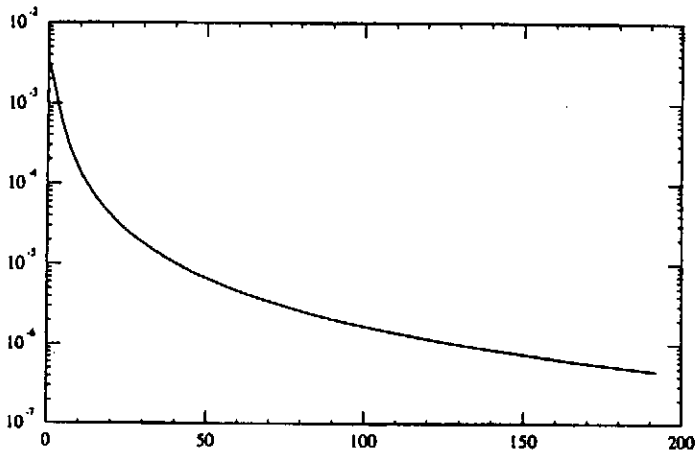

Figure 10 : Energy spread vs the phase loop gain

For an energy spread below 10^{-4}, we find that a minimal gain of 20 is required for both methods, but since the extra power increase is rather flat above this level, we set the phase loop gain around 50. Table 6 gives the quantities of interest for this loop gain for both methods and a gradient of 25 MV/m. Amplitude and phase errors are now defined as $\Delta V = Max(|V_{max} - V|, |V_{min} - V|)$ and $\Delta\phi = Max(|\phi_{max} - \phi|, |\phi_{min} - \phi|)$, and the initial detuning was adjusted to minimize the peak power.

method	$\Delta V/V$	$\Delta\phi$ (deg)	σ_E/E	$\Delta P_{peak}/P$ (%)	$\Delta P_{av.}/P$ (%)
self-excited loop	$0.5\ 10^{-5}$	0.38	$6.6\ 10^{-6}$	10.79	3.92
frequency jump	$0.5\ 10^{-5}$	0.37	$6.8\ 10^{-6}$	10.40	3.78

Table 6: Extra power for a phase loop gain $G_\phi = 50$

3.2. A chain of cavities with different Qs

In order to make the best possible use of the SC gradient capability, it would be advantageous to operate each cavity at its maximum field. Since the cavity tuning is not allowed to play with (see previous study), the easiest way of varying the cavity gradients in a chain fed by one klystron, is to change the external Qs from cavity to cavity. Even without Lorentz forces detuning however, a spread in external Qs, resulting from coupler tolerances or on purpose for having different cavity fields, will affect dramatically the amplitude error of the total voltage, because the source is not any more matched to the beam loads. We have therefore first to minimize this error by means of the incident power (P_g) and of the beam injection time (t_0), before attempting to close the feedback loops, which would result to a huge extra rf power. We study the case of an uniform spread in the individual accelerating gradients of a string of 16 cavities. The uniform gradient distribution spreads from 20 to 30 MV/m, with an average amplitude of 25 MV/m. According to Appendix B, we look simultaneously for the additional incident power (P_g) and the beam injection time (t_0) which minimize the amplitude error of the total cavity voltage without Lorentz forces detuning in a first step. For this ± 20 % accelerating field (or external Q) spread, the minimal amplitude error is obtained with an average extra power of about 15 % (230 kW instead of 200 kW per cavity) and a beam injection time of 0.59 ms (instead of 0.53 ms). The figure 11 shows the resulting total voltages, always without any Lorentz forces, with the nominal incident rf power of 200 kW per cavity (dotted line, the beam injection time has been delayed to recover the 25 MV/m at the end of the field rise time) and with the optimal klystron power and beam injection time values which minimize the fluctuations during the beam pulse (solid line).

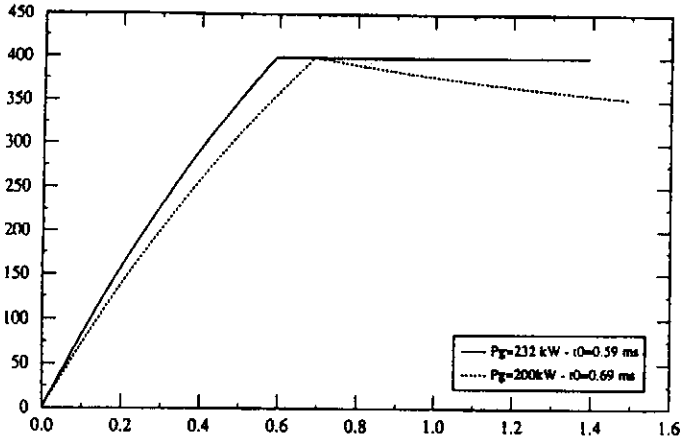

Figure 11 : total voltages with a 20 % gradient spread (without Lorentz forces)

Choosing these new generator power and beam injection time values, Table 7 gives the amplitude and phase errors of the total voltage during the beam pulse before feedback and with the Lorentz forces effects. We note that the amplitude errors are still large, leading to large energy spreads, even with the optimal values of the incident power and the beam injection time. The feedback loops gains were then optimized to reduce the energy spread to the 10^{-4} level without too prohibitive extra rf power. Table 8 gives the final errors and the needed rf power to add more, with gains of $G_A = 100$ and $G_\phi = 50$ for the feedback amplitude and phase loops, respectively.

method	$\Delta V/V$ (10^{-3})	$\Delta\phi$ (deg)	σ_E/E
self-excited loop	44.1	7.4	$1.2\ 10^{-2}$
frequency jump	52.8	6.7	$1.5\ 10^{-2}$

Table 7: amplitude and phase errors of the total voltage before feedback

method	$\Delta V/V$ (10^{-3})	$\Delta\phi$ (deg)	σ_E/E	$\Delta P_{peak}/P$ (%)	$\Delta P_{av.}/P$ (%)
self-excited loop	0.81	0.47	$2.23\ 10^{-4}$	17.76	6.17
frequency jump	0.81	0.47	$2.24\ 10^{-4}$	17.14	5.93

Table 8: Final errors and extra power with $G_A = 100$ and $G_\phi = 50$

It is worthwhile noting that the net additional power of 32 % peak (17+15) and 21 % average (6+15) needed for a string of 16 cavities fed by one klystron and assuming a spread of 20 % in accelerating fields is well above the extra power needed to counteract the Lorentz forces in case of one cavity per klystron (10.4 % peak and 3.8 % average, table 6). If the installed rf power does not meet this peak power requirement, the bunch to bunch energy spread will be worse.

4. MICROPHONICS EFFECTS

Up to now, since the cavity is freewheeling during the field rise time, the initial phase at the beginning of the rf pulse was assumed adjusted to the right value in such a way that the phase error is zero at the end of the field rise, when the beam is coming. The main effect of microphonics, because they change the cavity frequency, is to displace the rf phase with respect to the beam, assuming that the initial phase is fixed. The demand of rf power from the feedback loops is then huge. Assuming for example a detuning of 20 Hz due to microphonics, amplitude and phase feedback loops of 100 and 50, the peak rf power demand would be 1164 % ! with an initial phase adjusted for the unperturbated cavity frequency. Instead of having a fixed initial phase, we could think of a feedback system acting on this initial phase to recover a vanishing phase shift when the beam is coming. Unfortunately the frequencies of mechanical vibrations are expected to be around and above the TESLA repetition rate of 10 Hz, making a direct feedback unefficient. We could however take advantage of the fact that the errors coming from the Lorentz forces detuning are correlated whereas the errors coming from the microphonics detuning (jitter) are essentially uncorrelated. When it is essential to control the field for correlated errors, it would be a mere luxury to attempt to fight against uncorrelated errors, since their effects are much smaller (divided by the square root of the number of sections) at the end of the machine (see Appendix C for the expressions of the rms energy spreads). For the phase and amplitude references of the feedback loops, we therefore do not take fixed values any more, but the actual phase and amplitude of the field at the beam injection time, which then vary according to the mechanical vibrations. These signals can be easily recorded by means of a tracking-and-hold circuit. The figure 12 shows for example the phase error curves during the beam pulse for 3 cavity tunings, the optimal one and with a shift of ± 50 Hz around due to microphonics, giving a moderate extra peak power of 20 %, with amplitude and phase loop gains of 100 and 50.

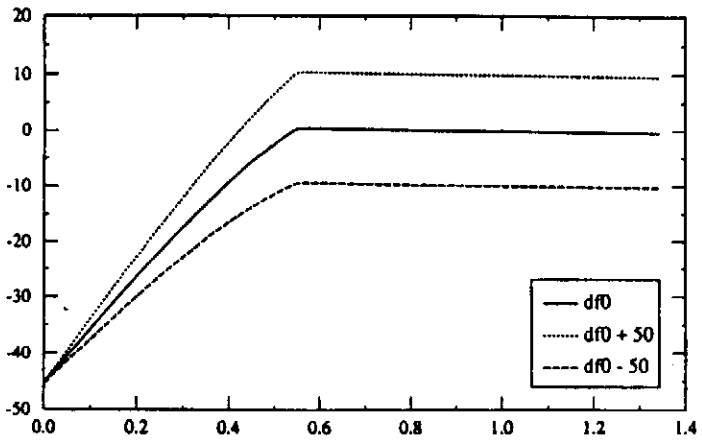

Figure 12 : Phase profiles for the optimal initial tuning and ± 50 Hz around

The table 9 summarizes the peak-to-peak correlated field errors within the beam pulse and the extra powers for these 3 cavity tunings.

dfo (Hz)	$\Delta V/V$ (10^{-4})	$\Delta\phi$ (deg)	$\Delta P_{peak}/P$ (%)	$\Delta P_{av.}/P$ (%)
264 (optimal)	0.1	0.38	11	4
264 + 50	0.2	0.5	20	6
264 - 50	0.2	0.5	20	6

Table 9: Field errors and extra powers with $G_A = 100$ and $G_\phi = 50$

Besides, this phase jitter of large magnitude (±10° for a detuning of ±50 Hz) gives a rms relative energy spread of about 2%, divided by the square root of the sections, which is not unfortunately the number of cavities, but the number of klystrons (625), due to the arrangement in strings of 16 cavities. The tolerance on the mean microphonics detuning is then around ± 20 Hz In conclusion, even with large phase jitter, these floating feedback references sets bounds to the extra rf power, while keeping the final energy spread to the 10^{-4} level.

REFERENCES

[1] A. Mosnier and O. Napoly, "Energy spread Induced in the TESLA Linac", TESLA Report 93-07

[2] A. Mosnier, "Dynamic measurements of the Lorentz Forces on a MACSE cavity", TESLA Report 93-09

[3] H. Henke, B. Littmann, "Mechanical Parameter Influence on the TESLA Cavity under Lorentz Forces", TESLA Report 93-12

[4] A. Mosnier, "Field Stabilization with Lorentz Forces", DAPNIA/SEA Note 93-03

APPENDIX A - SYSTEM'S EQUATIONS

The time equation for the voltage of a cavity driven by a generator of frequency ω_r and loaded by a beam current is given by

$$\ddot{V} + \frac{\omega_r}{Q}\dot{V} + \omega_r^2 V = \frac{\omega_r}{Q}(\dot{V}_g - \dot{V}_b)$$

All quantities oscillate with the frequency ω_r but we are interested in the evolution of the envelopes. The schematic drawing below shows the various voltages of the system involving the cavity, the generator and the beam.

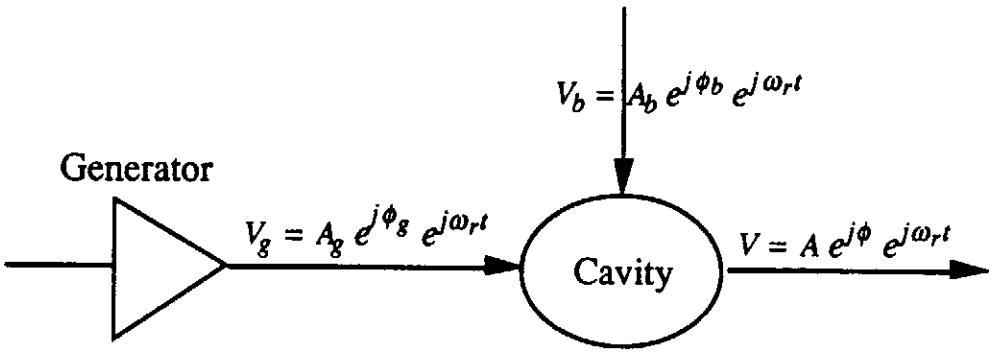

Assuming slow variations of the amplitudes and phases with respect to the rf period, the previous 2nd order equation reduces to the following 1st order equations

$$\begin{aligned} \tau\dot{A} &= A_g\cos(\phi-\phi_g) - A_b\cos(\phi-\phi_b) - A \\ \tau\dot{\phi} &= -\frac{A_g}{A}\sin(\phi-\phi_g) + \frac{A_b}{A}\sin(\phi-\phi_b) - \tau(\omega_r-\omega_c) \end{aligned} \qquad (1)$$

For a high coupling factor, the amplitudes of the generator and beam voltages are

$$A_g = 2\sqrt{R/Q\,Q_{ex}P_g} \quad \text{and} \quad A_b = R/Q\,Q_{ex}I_0$$

Furthermore, the Lorentz forces detuning is described by another 1st order equation

$$\tau_m\dot{\Delta\omega_c} = -\Delta\omega_c - 2\pi K A^2$$

where ω_c is the actual cavity frequency

$\tau = 2Q/\omega_c$ and τ_m are the electric and mechanical time constants.

A.1. Frequency jump method

During the field rise time, the generator frequency is locked to the cavity frequency by means of a Voltage Control Oscillator or equivalent circuit, which locks the phase of the generator to the phase of the cavity ($\phi = \phi_g$).

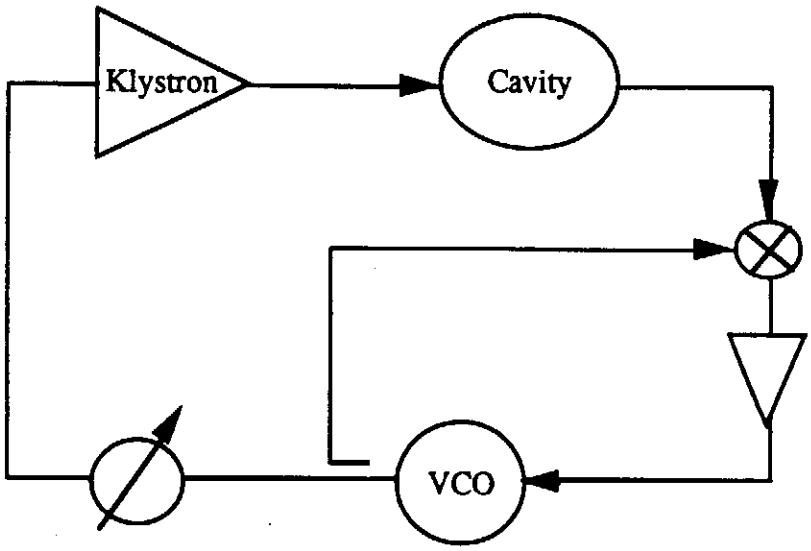

The equations (1) becomes simply

$$A(t) = A_g\left(1 - e^{-t/\tau}\right) \text{ and } \dot{\phi} = (\omega_r - \omega_c)$$

At the beam injection time, the generator frequency jumps to the fixed reference frequency ω_r . For a beam coming at the crest of the rf wave, the equations (1) are

$$\begin{aligned} \tau\dot{A} &= (A_g - A_b)\cos(\phi) - A \\ \tau\dot{\phi} &= -(A_g - A_b)\sin(\phi)/A - \tau(\omega_r - \omega_c) \end{aligned} \qquad (2)$$

A.2. Self-excited loop

The resonator is inserted in a self-excited loop, in such a way that the generator tracks the cavity frequency.

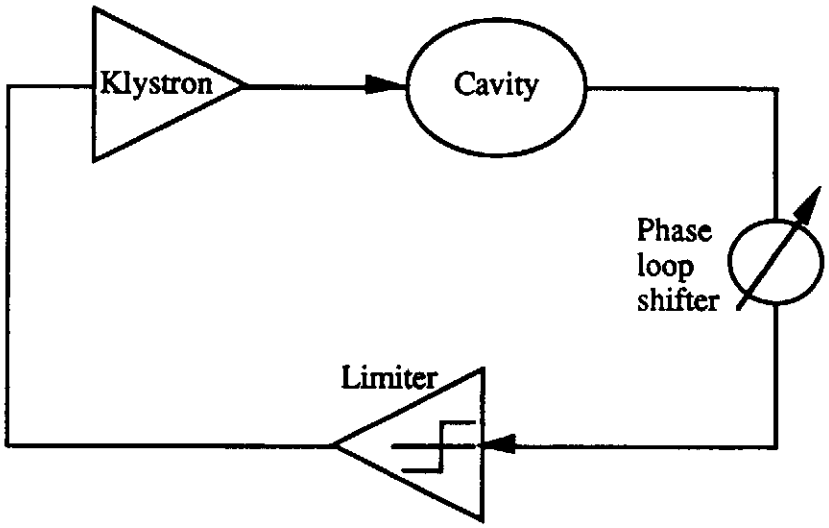

The behaviour is identical to the frequency jump method during the field rise time. During the beam pulse however, the phase of the generator is just the phase of the cavity, except for an error, called the loop phase shift θ_l.. The equations (1) become

$$\begin{aligned} \tau \dot{A} &= A_g \cos(\theta_l) - A_b \cos(\phi) - A \\ \tau \dot{\phi} &= -A_g \sin(\theta_l)/A + A_b \sin(\phi)/A - \tau(\omega_r - \omega_c) \end{aligned} \tag{3}$$

The loop phase shift is normally set to zero in order to drive the cavity at the resonance frequency.

A.3 N cavities driven by a single generator

The schematic drawing below shows for example the arrangement of several cavities in a self-excited loop

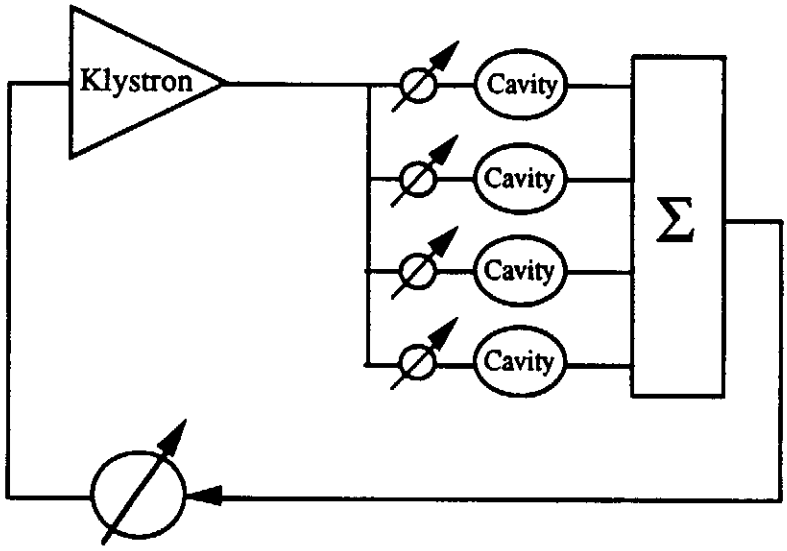

The system is now described by 3 N differential equations, related to the amplitudes and phases of the individual cavities.

$$\begin{aligned} \tau_i \dot{A}_i &= A_{g_i} \cos(\phi_i - \phi - \theta_l - \theta_i) - A_{b_i} \sin\phi_i - A_i \\ \tau_i \dot{\phi}_i &= -A_{g_i} \sin(\phi_i - \phi - \theta_l - \theta_i)/A_i + A_{b_i} \sin(\phi_i)/A_i - \tau_i (\omega_r - \omega_{ci}) \\ \tau_{mi} \dot{\Delta\omega}_{ci} &= -\Delta\omega_{ci} - 2\pi K_i A_i^2 \end{aligned}$$

where a global θ_l and individual θ_i loop phase shift have been allowed.

A last equation gives the amplitude and phase of the total voltage of the N cavities in terms of the individual cavity voltages

$$A\, e^{j\phi} = \sum_{i=1}^{N} A_i\, e^{j\phi_i}$$

A.4 the control system

To stabilize the field, the principle of a complex phase modulator is used. A in-phase signal and an out-of-phase signal are injected into the generator voltage, in proportion to the magnitude and phase errors. The figure below illustrates scematically the method

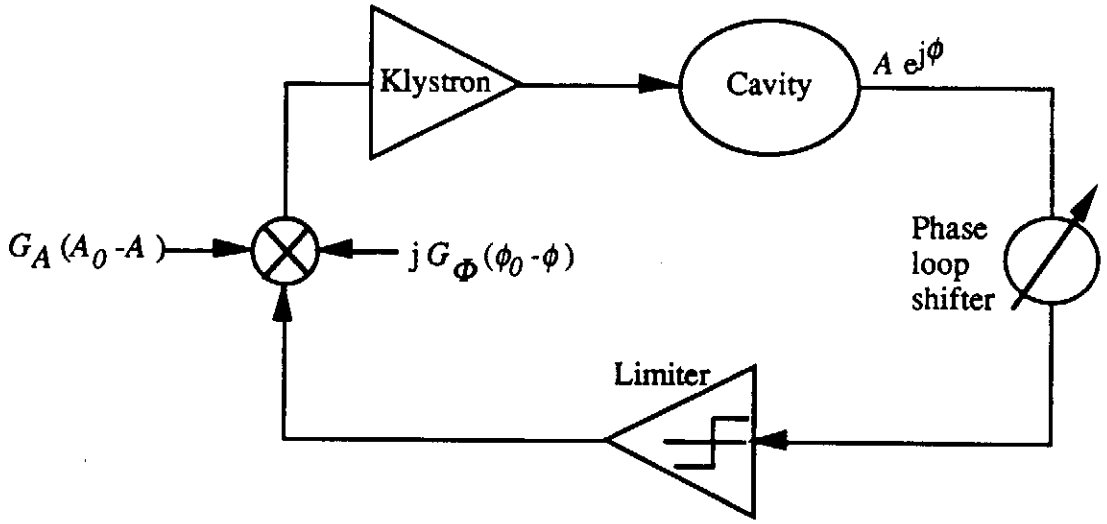

The amplitude of the generator voltage has to be replaced by

$$A_g \rightarrow A_g\,(1+\Delta A_p + j\,\Delta A_q)$$

with the in-phase and out-of-phase amplitudes given by

$$\Delta A_p = G_A(A_0 - A) \quad \text{and} \quad \Delta A_q = G_\phi(\phi_0 - \phi)$$

where A_0 and ϕ_0 are the amplitude and phase references

G_A and G_ϕ are the gains of the amplitude and phase feedback loops

For example, the equations related to the arrangement of several cavities in a self-excited loop and with feedback loops are given by

$$\tau_i \dot{A}_i = A_{g_i}\cos(\phi_i - \phi - \theta_l - \theta_i) + A_{g_i}\Delta A_p - A_{b_i}\sin\phi_i - A_i$$

$$\tau_i \dot{\phi}_i = -A_{g_i}\sin(\phi_i - \phi - \theta_l - \theta_i)/A_i + A_{g_i}/A_i\,\Delta A_q + A_{b_i}\sin(\phi_i)/A_i - \tau_i(\omega_r - \omega_{ci})$$

The additional power delivered by the klystron depends on the feedback loops gains and is the quadratic sum of the in-phase (active) and out-of-phase (reactive) rf powers :

$$\Delta P_g = \Delta A_p^2 + \Delta A_q^2$$

APPENDIX B - COUPLING FACTORS DISPERSION

Without Lorentz forces detuning, the variation of the voltage for the cavity i during the beam pulse is

$$A_i(t) = (A_{gi} - A_{bi}) + (A_{bi} - A_{gi}\, e^{-\frac{t_0}{\tau_i}})\, e^{-\frac{t-t_0}{\tau_i}}$$

where t_0 is the beam injection time

$A_{g_i} = 2\sqrt{R/Q\ Q_{ex_i} P_g}$ is the generator voltage

$A_{b_i} = R/Q\ Q_{ex_i} I_0$ is the beam induced voltage

$\tau_i = 2Q_{ex_i}/\omega_c$ is the electric time constant

When all cavities in the string are identical (parameters and gradients), the minimal power delivered by the source for a given gradient (optimal coupling) is obtained when all the rf power is absorbed by the beam, giving $A = A_b$

The accelerating field curve is then flat when the following relationship is satisfied

$$A_b = A_g\, e^{-\frac{t_0}{\tau_i}} \quad \Rightarrow \quad e^{-\frac{t_0}{\tau_i}} = \frac{1}{2}$$

When different cavity gradients with a single source are prescribed, the loads are no longer matched to the source and the total field profile during the beam pulse cannot be flat any more. A computer code was used to determine the source power and the beam injection time which minimize the fluctuations of the total accelerating voltage. The generator power P_g is swept and we look for the beam injection time t_0 which gives the minimal fluctuations (the external Qs must be calculated for each new set because the individual gradients are prescribed). The following plot shows the needed source power (in kW) against the fluctuation level of the total voltage for different widths of the gradient spread. About 230 kW per cavity (instead of 200 kW) are needed to reach amplitude errors of the order of 10^{-4}.

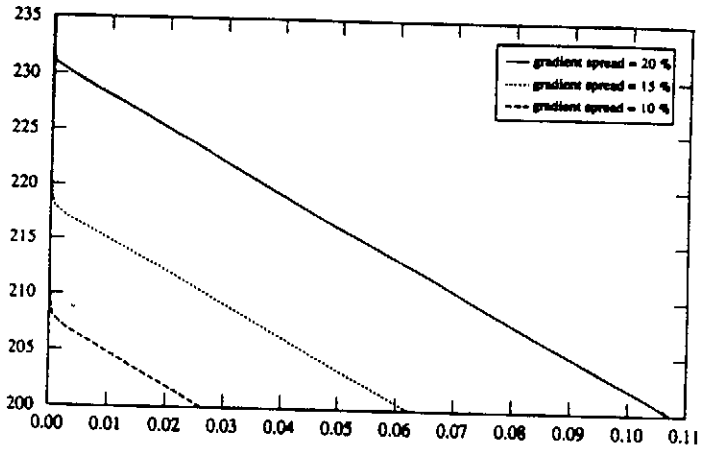

Needed source power (in kW) vs. the fluctuation level of the total voltage

APPENDIX C - ENERGY SPREAD FROM PHASE AND AMPLITUDE ERRORS

The voltage gain of a particle passing through the n^{th} cavity and the total voltage gain at the end of the linac are

$$V_n = V_0(1+\delta a_n)\cos(\phi_0+\delta\phi_n) \quad \text{and} \quad V_{tot} = \sum_{n=1}^{N} V_n$$

where V_0 and ϕ_0 are the nominal voltage amplitude and phase and

N is the number of cavities of the accelerator

δa_n and $\delta\phi_n$, the amplitude and phase errors of the rf voltage when a particle passes though the cavity, are random variables, characterized by the distribution functions $f(\delta a_n)$ and $g(\delta\phi_n)$.

When the errors are totally correlated (coming for example from the Lorentz forces), the total voltage gain can be written

$$V_{tot} = NV_0(1+\delta a)\left[\cos(\phi_0)\cos(\delta\phi)-\sin(\phi_0)\sin(\delta\phi)\right]$$

because $\delta a_1 = \delta a_2 = \ldots = \delta a_n = \delta a$ and $\delta\phi_1 = \delta\phi_2 = \ldots = \delta\phi_n = \delta\phi$

The average is then given by

$$\langle V_{tot}\rangle = NV_0\cos(\phi_0)\langle\cos(\delta\phi)\rangle$$

Performing the quadratic average, we obtain

$$\langle V_{tot}{}^2\rangle = N^2V_0{}^2\left(1+\langle\delta a^2\rangle\right)\left[\cos(2\phi_0)\langle\cos^2(\delta\phi)\rangle+\sin^2(\phi_0)\right]$$

The rms relative energy spread squared at the end of the linac is therefore

$$\frac{\langle V_{tot}{}^2\rangle - \langle V_{tot}\rangle^2}{\langle V_{tot}\rangle^2} = \frac{\left(1+\langle \delta a^2\rangle\right)\left[\cos(2\phi_0)\langle\cos^2(\delta\phi)\rangle + \sin^2(\phi_0)\right] - \cos^2(\phi_0)\langle\cos(\delta\phi)\rangle^2}{\cos^2(\phi_0)\langle\cos(\delta\phi)\rangle^2}$$

Assuming normal distributions for the amplitude and phase errors, the averages of the cosine functions become

$$\langle\cos(\delta\phi)\rangle = e^{-\frac{1}{2}\sigma_\phi^2} \quad \text{and} \quad 2\langle\cos^2(\delta\phi)\rangle = 1+\langle\cos(2\delta\phi)\rangle = 1+e^{-2\sigma_\phi^2}$$

For small errors, the rms relative spread is then

$$\sigma_E/E \approx \frac{1}{\cos(\phi_0)}\sqrt{\frac{1}{2}(1+\cos(2\phi_0))\sigma_a^2 + \frac{1}{2}(1-\cos(2\phi_0))\sigma_\phi^2 + \frac{1}{4}(3\cos(2\phi_0)-1)\sigma_\phi^4}$$

When the bunches are at the crest of the rf wave ($\phi_0 = 0$), the previous expression becomes simply

$$\sigma_E/E \approx \sqrt{\sigma_a^2 + \frac{\sigma_\phi^4}{2}} \qquad \text{(correlated errors)}$$

On the other hand, when the errors are uncorrelated (coming for example from the mechanical vibrations), the proper statistical average yields the well-known result that the previous expressions have to be divided by the square root of the number of sections

$$\sigma_E/E \approx \sqrt{\sigma_a^2 + \frac{\sigma_\phi^4}{2}} \Big/ \sqrt{N} \quad \text{(uncorrelated errors)}$$